Smart Sensor Arrays

Maik-Ivo Terasa, Leonard Siebert, Pia Holtz, Sören Kaps, Oleg Lupan, Jürgen Carstensen, Franz Faupel, Alexander Vahl, and Rainer Adelung

Abstract Sensors play a crucial role in our everyday life and will become more and more demanded with the transition towards smart cities and the "Internet of Things" with the result of an ever-increasing energy demand. Thus, the research of improving the energy efficiency of sensor systems has started to move towards edge computing and neuromorphic engineering while at the same time additive manufacturing has gained increasing attention as a means for a rapid, scalable fabrication of functional devices yet with huge design freedom and quick iteration cycles during the development phase. In this chapter the junction of pre-designed components with self-organizing material systems for the facile fabrication of sensor devices via direct ink writing is demonstrated. As examples 3D-printed $CuO/Cu_2O/Cu$- and CuO/Fe_2O_3

M.-I. Terasa (✉) · L. Siebert · P. Holtz · S. Kaps · O. Lupan · J. Carstensen · R. Adelung
Functional Nanomaterials, Department of Materials Science and Engineering, Kiel University, Kaiserstraße 2, 24143 Kiel, Germany
e-mail: mate@tf.uni-kiel.de

L. Siebert
e-mail: lesi@tf.uni-kiel.de

P. Holtz
e-mail: piah@tf.uni-kiel.de

S. Kaps
e-mail: ska@tf.uni-kiel.de

O. Lupan
e-mail: ollu@tf.uni-kiel.de

J. Carstensen
e-mail: jc@tf.uni-kiel.de

R. Adelung
e-mail: ra@tf.uni-kiel.de

F. Faupel · A. Vahl
Multicomponent Materials, Department of Materials Science and Engineering, Kiel University, Kaiserstraße 2, 24143 Kiel, Germany
e-mail: ff@tf.uni-kiel.de

A. Vahl
e-mail: alva@tf.uni-kiel.de

M. Ziegler et al. (eds.), *Bio-Inspired Information Pathways*, Springer Series on Bio- and Neurosystems 16, https://doi.org/10.1007/978-3-031-36705-2_11

acetone gas sensors are shown, as well as how the decoration of metal-oxide semiconducting sensor materials with noble metallic nanoparticles can enhance the sensor properties with respect to sensitivity, selectivity and stability. Finally, the assembly of conductive bridges between electrodes stimulated by voltage pulses is introduced as an approach towards facilitating the self-organization of neuromorphic circuits.

Keywords Memsensors · Metal-oxide semiconductor sensors · 3D-printing · Direct ink writing · Triggered assembly

1 Introduction

Sensors are a key component of our everyday life. They are used to detect changes in the environment that are hazardous or of interest otherwise. Living organisms use environmental stimuli triggering their sensory systems as inputs to adapt their behaviour to the environmental surrounding, e.g., for finding food or evaluating danger. In this regard biological systems have been evolutionary optimized to be most energy-efficient since this is a crucial advantage for survival. An example is the adaptation to a permanent background stimulus [1]. The sensory system changes such, that the response to an excitation decreases, if the stimulus does not change over a long period of time. For example, a human eye in a dark room contracts its pupil when suddenly the light is turned on, accommodating to the new lighting situation, thus allowing the eye to see normally after adaptation. However, technical advances presented humanity with new challenges surpassing the capacities of humans' natural sensors. Technical sensors have been developed to compensate or extend the capabilities of the human body, especially for security and health applications e.g. monitoring the concentration of harmful radiation or toxic gases, but also for a wide variety of purposes like magnetic field sensors, CCD-sensors or mechanical sensors. With the ever growing number of electronic devices and the development towards the "Internet of Things" and "Smart Cities" the number of deployed sensors will increase significantly in the future and a crucial aspect is the growing energy demand, that accompanies this development [2–4]. However, biological systems are remarkably efficient, when it comes to data acquisition and processing. This has inspired research to mimic the way they achieve their great energy efficiency. A prominent approach for higher energy efficiency to account for the growing energy demand is overcoming the von-Neumann bottleneck by using features of edge computing and neuromorphic engineering, i.e. decentralizing computing logic and memory to reduce the power consumption of communication between them and diminish the need for data transmission to a central server [5–8]. In the following sections, various concepts will be discussed, that advance the research in sensor technology to account for the demand of efficient, scalable, specialized and smart sensor devices. At first the concept of the memsensor will be introduced, which is a novel junction of a sensor with memristive components yielding additional unique abilities, such as adaptation to a permanent background stimulus. It will be discussed with respect to an equivalent circuit model

and a ZnO needle as an example system. When it comes to the fabrication of sensor devices, most processes rely on micro-patterning by lithography and physical or chemical vapour deposition techniques, which are inherently demanding with respect to workplace and material quality [9, 10]. Here, additive manufacturing (AM), which is based on inexpensive and highly available equipment, is discussed as a means of fabrication for sensor devices. The AM approach provides huge design freedom with respect to sensor materials and shape as well as quick iteration cycles making it a valuable tool for research and development of sensor devices. Metal-oxide semiconductor (MOS) microparticles are showcased as sensor materials printable by direct ink writing (DIW) and the enhancement of their sensor performance by decoration with metallic nanoparticles is discussed. In the last section, the dynamic establishment of conductive interconnections between electrodes at the microscale in a liquid matrix is introduced by the example of copper electrodes in an electrolyte of dimethyl sulfoxide (DMSO) and methylene blue (MB), which serves as a first step towards expanding brain-inspired plasticity mechanisms to a larger scale.

2 Smart Sensors

This chapter evolves around sensor devices that belong to the category of semiconducting metal oxide micro- and nanostructures, such as CuO, TiO_2, ZnO. Such materials are commonly used for sensing applications, for example as photon sensors or gas sensors. While photon sensing involves a considerable fraction of the material, depending on the photon penetration depth in the material, gas sensing is strongly related to the adsorption and desorption of molecular species onto the sensor surface and therefore can be considered as a surface phenomenon. Interestingly, there is a considerable overlap between materials used for MOS sensors and memristive devices that rely on the valence change mechanism upon migration of oxygen vacancies. This implies, that if manufactured in a proper way, a single device can intrinsically unify the inherent functionalities of sensors and memristive devices, namely the stimulus dependent resistance and the controllable switching between resistance states. This section will elucidate the properties of memsensors that arise upon the junction between memristive switching and stimulus sensing. In order to obtain memsensitive properties, an important requirement is that the active material must be accessible to the chosen external stimuli. This requirement strongly depends on the type of stimulus—while gas sensors need a direct contact of the gas species to the sensor surface, other stimuli like photons or magnetic fields may also potentially penetrate through matter. This requires the top electrodes of vertically sandwiched devices to be chosen carefully or to be additionally structured. Another option is the use of lateral structures, like micro- or nanowires that are in direct contact with the surrounding medium. An example for such horizontal structure are ZnO microneedles. A ZnO needle with a diameter in the μm range and a length in the cm range is shown in Fig. 1a. Details on the manufacturing are reported elsewhere [11].

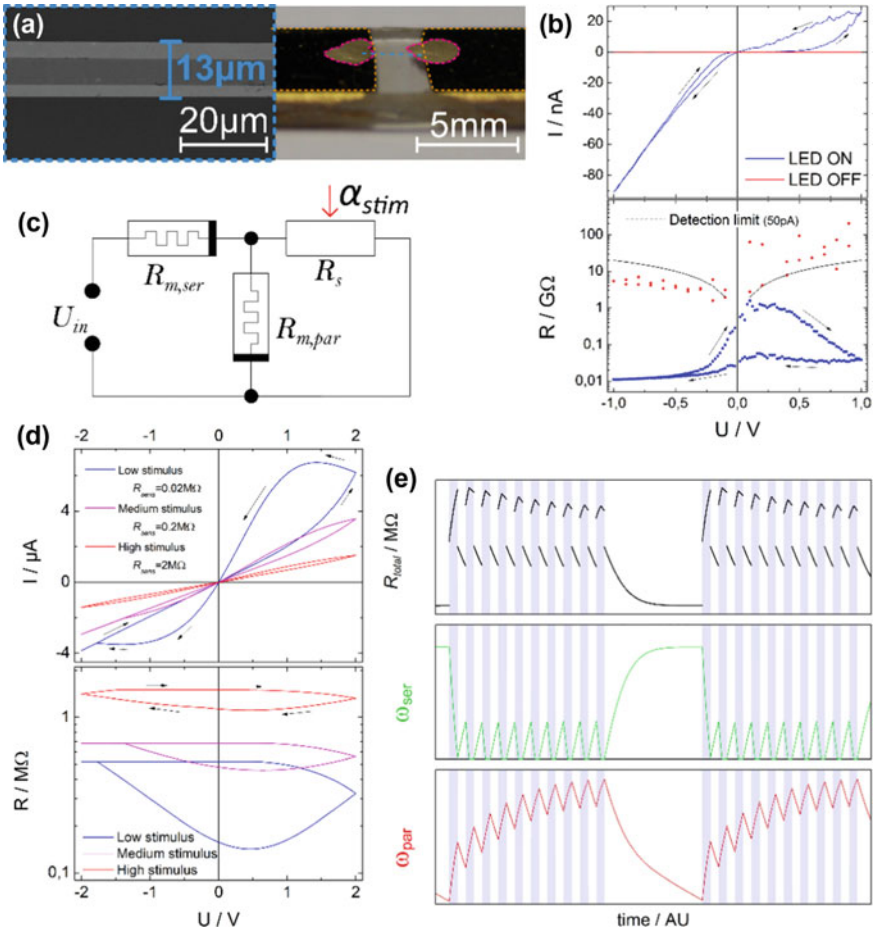

Fig. 1 A ZnO microrod device **a** as a memsensor device prototype is capable of showing stimulus dependent hysteresis. **b** An equivalent circuit **c** with three components was used to model stimulus dependent hysteresis **d** and adaptation of the resistance of a memsensor device to an external stimulus **e**. In case of amplitude adaptation **e**, the resistance response (black) of the modelled memsensor decreases with each consecutive stimulus pulse decreases, which is based on the slower change in the internal state of the parallel resistor (red) than the serial resistor (green) [11]. Reprinted with permission from [11]

The electrical resistance of a ZnO microneedle exhibits a strong dependence on the illumination by UV photons. Interestingly, IV hysteresis measurements of the ZnO needle device show an UV dependent hysteresis, which is depicted in Fig. 1b. While the IV characteristics in the dark state do not show a pinched hysteresis and in general exhibit an overall very high resistance, under UV illumination there is a pronounced pinched hysteresis. Accordingly, the device requires the UV stimulus to show memristive switching. A junction between memristive switching and sensing

has been reported for a variety of devices [12–14]. To understand the phenomenon of stimulus dependent hysteresis and study the potential properties of memsensors, a simple three-component model was proposed (Fig. 1c), that allows to investigate the interplay between memristive switching and sensing [11]. Within this model, in first approximation, the sensor response is assumed to be immediate, while the memristive devices can occupy a smooth transition of resistance states between a fixed LRS and HRS. As such, stimulus dependent hysteresis at a given voltage window was reproduced, as depicted in Fig. 1d. In the context of the model, the occurrence of stimulus-sensitive hysteresis originates from the difference in potential drop over the serial memristive element, that leads to a significantly more pronounced hysteresis in the illuminated state. As an additional memsensor feature that goes beyond the inherent features of sensors and memristive devices, amplitude adaptation to a constant stimulus was modelled (Fig. 1e), mainly governed by the different rate of change in inner state for both memristive devices. This predicts that the junction of sensing and memristive switching has the potential to create smart sensor devices, that show bio-inspired features like adaptation.

3 Additive Manufacturing of Sensors

Self-organized systems are shaped by mechanisms of positive and negative feedback, meaning that occurring "positive" events make them more likely to occur again, while "negative" events become more unlikely. This feedback-driven dynamic makes the system generally robust against fluctuations and will lead it towards its most desirable state, defined by the feedback mechanisms. While self-organization is an important feature of efficient bio-inspired systems, there are many examples for parts of biological systems that are formed by a fixed pattern because they often serve a specific purpose e.g. the eye as a means of perceiving visual information. Such pre-designed patterns generally make up every technical device, though when used in dynamic self-organized systems in an emerging concept like neuromorphic computing it is advisable to have fast iteration speed during the development stage, to be able to adapt and optimize the design quickly. At the same time as much design-freedom as possible should be maintained with respect to the geometry, material or composition of parts. In this context the field of additive manufacturing (AM) has shown to offer beneficial features for rapid design and production of prototypes of both structural and functional components. Traditional manufacturing of parts is mostly subtractive e.g. milling, drilling, etc., where material is removed from the part until it is shaped as intended. This creates a substantial deal of waste while it becomes more difficult and thus expensive the more complex the shape of the part is. In contrast to this top-down approach, additive manufacturing (AM) works "bottom-up" by assembling the final part out of small fractions. The most common way is by stacking thin layers of material on top of each other to create 3D objects (see Fig. 2a). For the deposition of material for each layer there are several different approaches available, depending on the matrix material and specifications of the

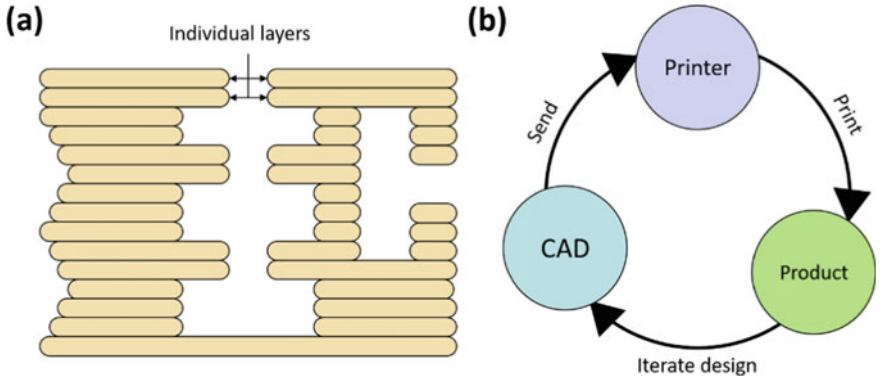

Fig. 2 Benefits of additive manufacturing: **a** The bottom-up approach (i.e. stacking layers of material) facilitates more complex geometries, like undercuts in the center of a piece, that would be difficult to manufacture by traditional machining. **b** Quick iteration cycles are made possible by directly linking the design and fabrication steps

part like minimum feature size. Processes like fused deposition modelling (FDM) melt a thermoplastic filament and extrude it through a nozzle to deposit the material, while stereolithography (SLA) is based on the photopolymerization of thin layers of liquid resin. Metal parts can be produced by selective laser sintering (SLS) or the conceptually similar selective laser melting (SLM), which heat up a metal powder to sinter or melt the grains together [15, 16]. Most commonly object data is provided by digital 3D object files, e.g. in the STL-format, created by computer aided design (CAD) programs. Object design and fabrication are direct subsequent steps, as seen in Fig. 2b. A designer has both large freedom with respect to geometry and materials, while also being able to work through a part's iteration cycles quickly. This led to AM also being considered "rapid prototyping" making it a perfect tool to use in research and development.

3.1 Direct Ink Writing of Microparticles

Direct Ink Writing (DIW) is a subtype of AM, where an ink composed of a carrier fluid and colloidal particles with high filler content is extruded onto a substrate through a moveable nozzle. The carrier fluid consists of a volatile solvent and possibly a polymeric binder. After extrusion the solvent evaporates and the ink solidifies. While this technology already has been around for many years in the form of inkjet printers for digital images it also got more recent attention as means for AM by depositing ceramic particles via the ink [17–19]. DIW allows printing of any materials in powder form, particularly materials that are not suitable for other additive manufacturing methods or that have complex particle morphologies. This also includes functional particles like tetrapodal ZnO (t-ZnO, [20]), which expands the capabilities of AM

from purely structural parts towards functional or composite components. However, the rheological properties of the ink are crucial for the reliable fabrication with DIW. The ink must remain homogeneous and flow evenly to avoid defects or aberrations in the print. Colloidal suspension inks are based on a carrier fluid and one or more species of suspended micro- and/or nanoparticles. In some cases, a polymeric binder has to be added to the solvent increasing the inks viscosity. E.g. if the particles are too large to stay suspended in the pure solvent, a polymeric binder is added to increase the viscosity preventing the particles from sedimenting. Furthermore, complex shaped particles like t-ZnO form highly porous, tangled agglomerates. A high viscosity ink is necessary to exert the shear forces required to move the particles, otherwise the solvent would flow through the pores separating from them. The carrier fluid commonly solidifies either by evaporation of the solvent (e.g. for the systems H_2O/PEG or EtOH/PVB) or by a chemical reaction (e.g. silicones). Once solid it can either persist as a structural matrix for the particles or be removed by thermal or chemical decomposition. Especially for functional microparticles it is commonly desired to remove the binder to create interfaces to other external species, like gases or light, or create percolating or dense structures approximating the properties of the bulk material e.g. the electrical conductivity.

3.2 EtOH/PVB as a Carrier Fluid

Using ethanol (EtOH) as a solvent and polyvinyl butyrale (PVB) as a polymeric binder has shown to yield interesting possibilities, which are further enhancing the flexibility of DIW for micro- or nanoparticle based components and can possibly be transferred to other similar systems as well. An EtOH/PVB based ink can be printed on a glass substrate (see Fig. 3a). Since PVB is a hydrophobic polymer, submerging the glass substrate in H_2O makes the printed material detach from the glass (see Fig. 3b). The result is a flexible free-standing structure, which in itself already opens new possibilities towards prints that can be folded to create 2.5-dimensional designs. In addition, if slightly wetted with EtOH again, the print can be re-attached to any suitable surface, including round or complex ones, on which printing and most other deposition techniques (e.g. sputter deposition) are unfeasible or even impossible, dramatically increasing the applicability of printed components (see Fig. 3c). Moreover, with a high-power laser instead of traditional unlocalized heating, the heat treatment process can be controlled precisely in terms of localization and power transfer. Using a 100 W CO_2 laser two main goals have been achieved: (1) With low power output, a gentle milling of a thin portion polymeric binder has been performed on a single layer print. Without damaging the embedded microparticles, the top portion of the layer has been stripped of its polymeric binder, exposing the functional particles, while keeping the bottom portion of the binder as mechanical support Fig. 3d. Even after the laser milling process the print could still be detached from the substrate. By combining inks of t-ZnO and CNTs an all-printed freestanding sensor device has been fabricated with this method, as shown in Fig. 3e. The geometric and mechanical

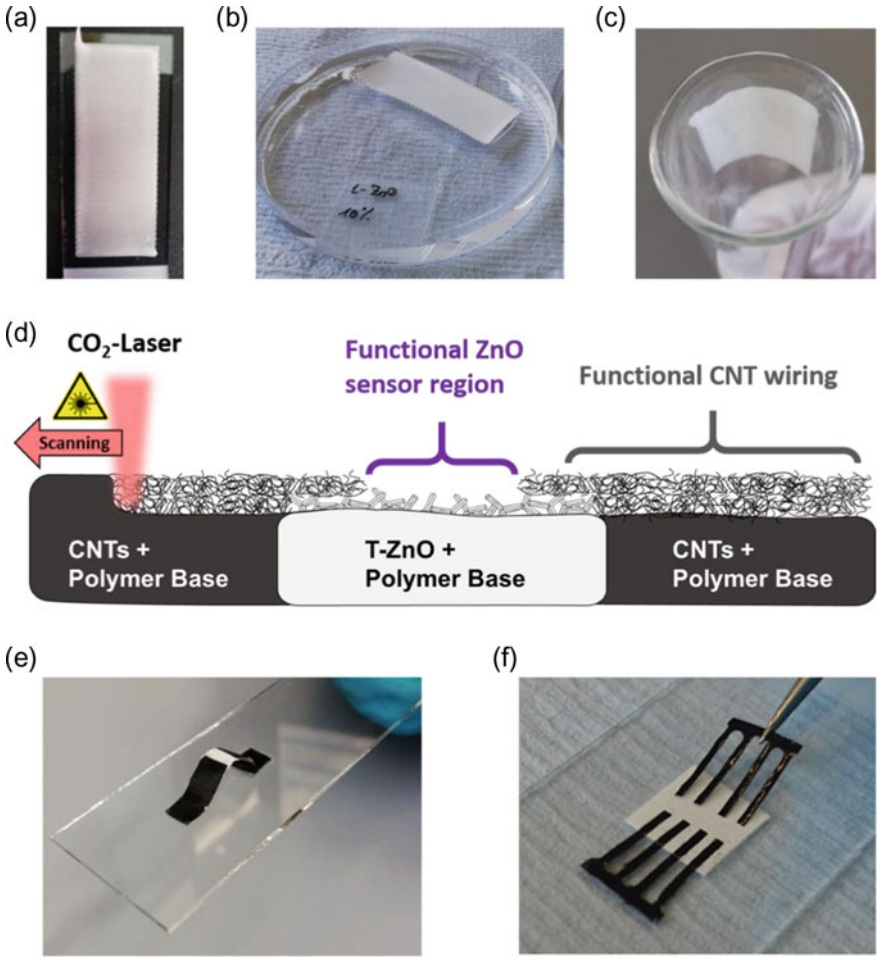

Fig. 3 **a** An as-printed layer of an ink of EtOH/PVB with t-ZnO as functional particles. **b** Submerging the glass substrate in water will make the printed layer delaminate. **c** The delaminated print can be re-attached conformably to round or complex surfaces. **d** Schematic of the gentle laser milling process. It allows for precise stripping of thin layers of polymer to expose the functional particles, while keeping a base of polymer for structural stability. **e** A free-standing all-printed UV-sensor composed of CNT-ink as wiring and t-ZnO as the sensor component. The print has been laser milled to expose the ZnO enabling its sensor functionality. **f** Separately printed and delaminated CNT- and ZnO-prints being assembled freely by slightly wetting the junctions with ethanol

flexibility makes such sensor devices a great candidate for components in electronic skin applications [21, 22]. Additionally separately printed parts can be assembled freely by wetting them at the respective junctions with ethanol (see Fig. 3f) or be stored as well as processed mechanically e.g. by cutting, allowing for production of stock or modular designs. (2) With higher power output a localized oxidation of metal particles has been accomplished, leading to precisely located metal/metal-oxide/metal interfaces, which is a promising starting point for simple and accessible, yet precise and scalable fabrication processes of MOS sensor devices.

3.3 High-Viscosity DIW Setup

The Chair for functional Nanomaterials at Kiel University has established a custom-built DIW setup for printing with inks of high viscosities, which is depicted in Fig. 4a. It's extrusion unit is able to exert high pressures up to 40 bar on the ink via a steel piston driven by a geared stepper motor. The ink reservoir is a commercially available polypropylene (PP) syringe encased in an aluminium shell to prevent expansion of the PP during extrusion. The extrusion nozzle is a conical syringe tip with an orifice diameter of 100 µm to 840 µm. The nozzle size determines the spatial resolution of the print, since a smaller diameter yields thinner lines and thus finer features. But at the same time it limits the size, morphology and fill factor of the printable microparticles. E.g. tetrapodal ZnO particles (t-ZnO) with an arm length of 25 µm or more have shown to clog nozzles with 100 µm diameter at higher fill factors of more than 10 wt% due to the tendency of the tetrapods to become tangled. In addition, the print bed is heatable and a 3 W computer controlled blue laser is pointed at the printing spot for precise localized heating. Figure 4b shows a selection of microparticles, that have been printed with this setup. The setup has been used to print all devices presented here and in Sect. 3.4.

3.4 Gas Sensors by DIW

Semiconducting metal oxides (MOS) have shown to be a superior material class for gas sensing applications, which are essential in the fields of workplace security, healthcare or environmental monitoring [23]. The mechanism of gas sensing is commonly attributed to the ad- or desorption of molecules on the solid-gas interface of the sensing material changing its electronic landscape, where oxygen is discussed as the most popular surface adsorbant species. Oxygen adsorbs to the surface of MOS by binding electrons from the conduction band:

$$O_2 + e^- \rightarrow O^-_{2(ad)}$$

In a n-type semiconductor this creates a high resistance electron depletion region narrowing the conduction channel, whereas in a p-type semiconductor a hole accumu-

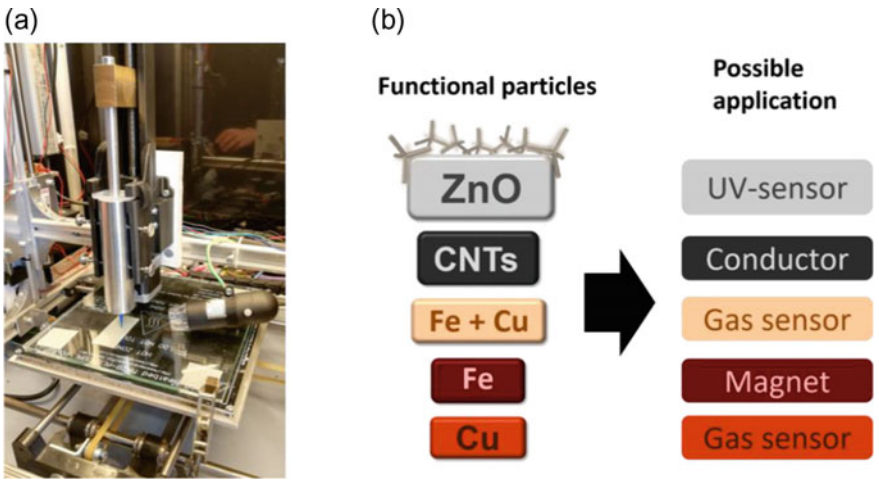

Fig. 4 **a** Photograph of the custom-built high-viscosity ink printing setup. **b** A selection of microparticle species that have been printed with the setup, as well as possible applications for each.

Table 1 Composition of the functional inks for MOS sensor devices

Sensor	$CuO/Cu_2O/Cu$	$CuO:Fe_2O_3$
Carrier fluid	Deionized H_2O	Ethanol
Polymeric binder	Polyethylene glycole	Polyvinyl butyrale
Microparticles	Copper (15–25 μm)	Copper (15–25 μm) + Iron (40–60 μm)

lation layer (HAL) with lower resistance is created. The sensor response is most commonly discussed in the context of chemical reactions or desorption of surface oxygen decreasing either the electron depletion layer or the hole accumulation layer. The acetone content of human breath has been shown to be significantly increased for individuals with diabetic ketoacidosis [24]. Thus acetone breath sensing is a promising tool for non-invasive diagnosis and monitoring of diabetic patients, with the aim for inexpensive, portable and broadly available sensor devices, giving patients cheaper and safer healthcare options, compared to conventional blood tests [25]. Acetone gas sensors based on self-organized MOS nanostructures, namely $CuO/Cu_2O/Cu$- and Fe_2O_3/Fe-nanospikes, have been manufactured via DIW and subsequent thermal annealing [26, 27]. The composition of the respective inks can be found in Table 1.

Ink lines have been printed on glass substrates with deposited gold contacts (see Fig. 5a–d). The prints have been annealed at 425 °C for 2 h ($CuO/Cu_2O/Cu$) and 4 h ($CuO:Fe_2O_3$) respectively, which served as means of binder removal as well as oxidation of the microparticles.

During oxidation self-organized spikes of metal oxide have grown outwards from the particles, significantly increasing their surface area and generating new heterojunctions between particles, as indicated in the micrographs in Fig. 6a–d. Both the

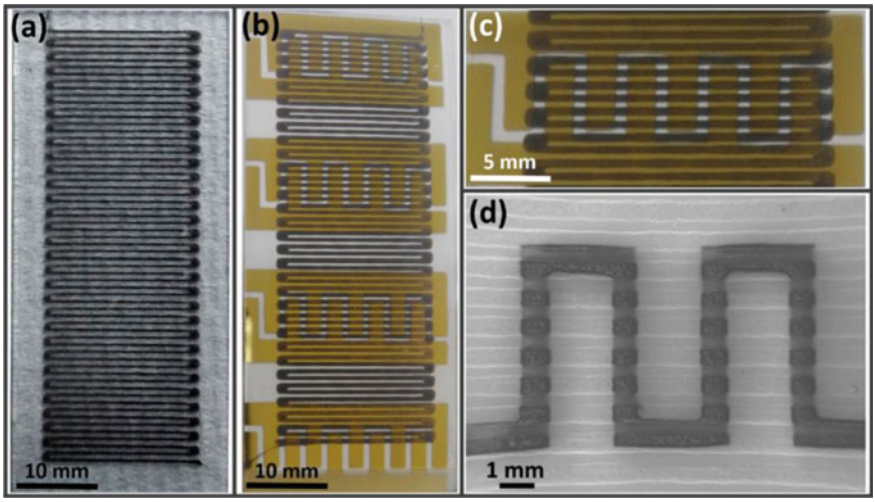

Fig. 5 Images of meandering printed ink lines: **a** Directly after printing. **b** After deposition of gold contacts. **c** Close-up of a single sensor element. **d** SEM micrograph of a sensor element. Reprinted with permission from [27]

CuO and the CuO:Fe_2O_3 sensors showed great selectivity and sensitivity to acetone vapours at an operating temperature of 300 °C or higher (see Fig. 6e+f).

The proposed sensing mechanism is the reaction of acetone with adsorbed surface oxygen:

$$CH_3COCH_3(ads) + 8O^-(ads) + 8h^+ \rightarrow 3CO_2 + 3H_2O$$

Since CuO is a p-type semiconductor the sensor response is based on the reduction of the HAL. In the case of CuO:Fe_2O_3 sensors besides the charge accumulation/depletion effect, the interfaces between CuO and Fe_2O_3 nanospikes form p-n-junctions that are proposed to increase in resistance by adsorbed acetone providing an additional potential barrier. These examples showcased that the technology of DIW is perfectly suitable for the design and production of sensing devices. Any species and even combinations of microparticles with sensing properties can be deployed with great geometric freedom, while allowing one to print on pre-designed circuit boards or substrates for immediate integration.

3.5 Enhancing Sensor Properties by Decoration with Noble Metal Nanoparticles

The gas sensing performance of MOS sensors with respect to sensitivity, stability or selectivity can be enhanced by doping as well as decoration with metallic nanoparticles. To give an example, ZnO as a H_2 sensor is considered. ZnO nanowires (a

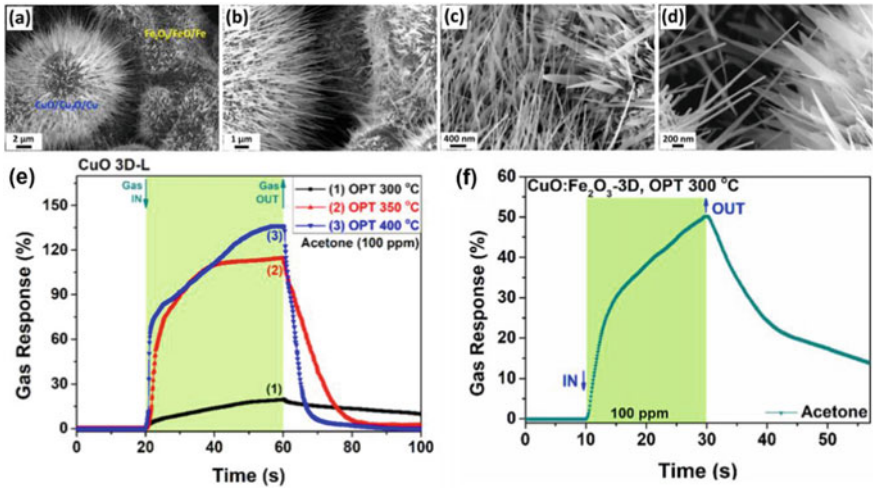

Fig. 6 SEM micrographs of the Cu and Fe microparticles after heat treatment. **a–d** Interface between the $CuO/Cu_2O/Cu$- and $Fe_2O_3/FeO/Fe$-nanospikes at different magnifications. **e** Gas response of 3D-printed CuO sensor to 100 ppm acetone vapor. **f** Gas response of $CuO:Fe_2O_3$ sensor to 100 ppm acetone vapor. Reprinted with permissions from [26, 27]

n-type semiconductor) are showing H_2 detection capabilities. A model proposed for the H_2 sensing mechanism while exposed to ambient air is based on the reaction of incoming H_2 molecules with the adsorbed oxygen to H_2O releasing electrons into the bulk during this process and thus decreasing the electron depletion region: [28]

$$H_2 + \tfrac{1}{2}O^-_{2(ad)} \rightarrow H_2O + \tfrac{1}{2}e^-$$

Though, such sensors are influenced as well by ambient parameters like relative humidity (RH), so that it is beneficial for the sensor performance to alleviate the response to changing conditions [29]. ZnO nanowires that have been decorated with Au nanoparticles (AuNP) have shown a significantly reduced susceptibility to changes in RH between 30% and 85% [30]. The tentatively proposed sensing mechanism for AuNP decorated ZnO nanowires extends the one for pure ZnO wires by taking into account the AuNP/ZnO interface (see Fig. 7). Due to the higher work function of the AuNP (Φ_{Au} = 5.1 eV, $\Phi_{ZnO} = 4.5$ eV) electrons flow from the bulk to the interface resulting in Schottky barriers at the Au/ZnO interface thus further enlarging the electron depletion region.

The water desorbs by the heat of the exothermic reaction and by the release of electrons the electron depletion layer is reduced. The higher sensor response for Au NP decorated ZnO is attributed to the larger depletion layer around the Au NP and the induced Schottky barriers, which result in a stronger modulation of the conduction channel [31]. The effect of doping and nanoparticle decoration of MOS sensors has been studied for a wide variety of material systems. An overview of examples is given in Table 2.

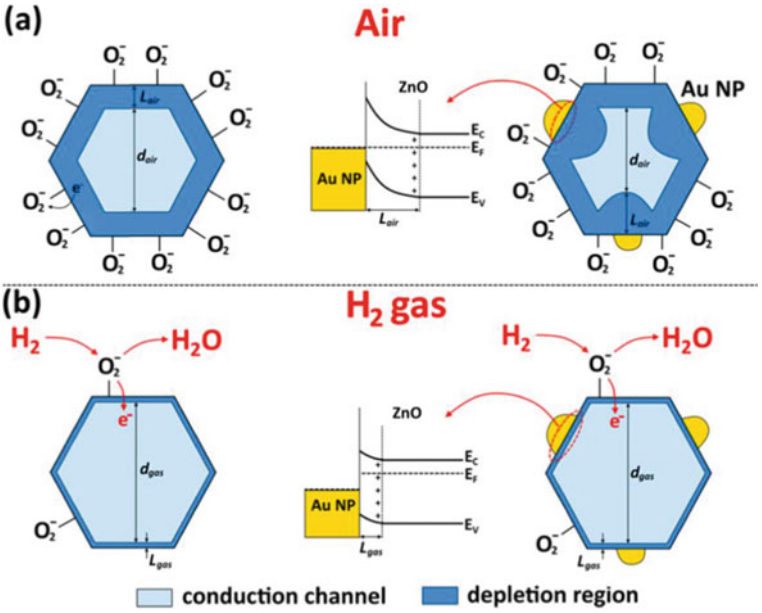

Fig. 7 Proposed mechanism for the gas-sensing of noble nanoparticle decorated ZnO nanowires. **a** Under ambient air. **b** Under exposure to H_2 gas. Reprinted with permission from [31]

Table 2 Overview over the effect of doping and nanoparticle decoration on gas sensor properties for various material systems

Base system	Nanoparticles	Effect	References
ZnO:Fe	AgO/Ag	Enhanced sensitivity to ehanol vapor	[32]
ZnO:Ag	Ag	Enhanced humidity stability	[33]
ZnO:Ag	AgAu	Enhanced sensitivity towards VOCs	[34]
ZnO:Ag	AgPt	Enhanced selectivity for hydrogen	[34]
TiO_2	Ag, Au, AgAu, AgPt	Enhanced selectivity for various gases	[35, 36]
ZnO:Eu	Pd	Decrease of working temperature for hydrogen sensing to RT	[37]
ZnO:Pd	PdO	Enhanced selectivity and sensitivity to hydrogen gas	[38, 39]
SnO_2	Zn_2SnO_4	Enhanced sensitivity to ethanol at RT	[40]

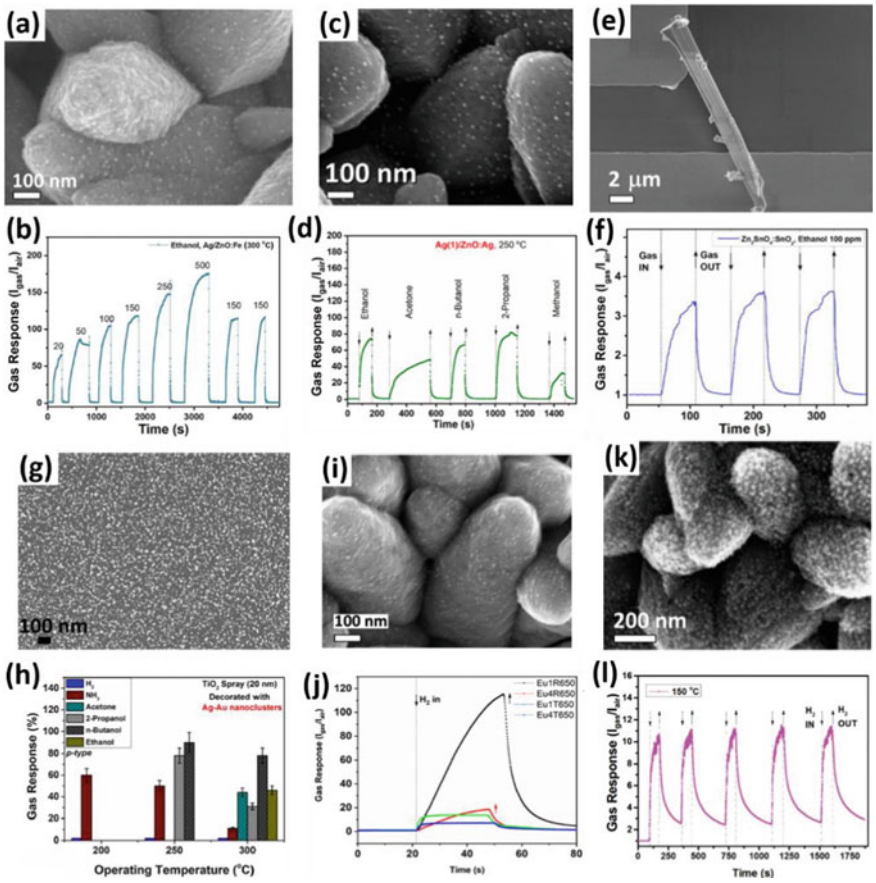

Fig. 8 Collection of doped and/or surface functionalized MOS based gas sensors. For each system an SEM micrograph as well as a characteristic gas sensor measurement is shown: **a+b** Fe doped ZnO decorated with Ag NP [32]. **c+d** Ag doped ZnO decorated with Ag NP [33]. **e+f** SnO_2 decorated with Zn_2SnO_4 NP [40]. **g+h** TiO_2 thin film decorated with AgAu NP [36]. **i+j** Europium doped ZnO decorated with Pd NP [37]. **k+l** Pd doped ZnO decorated with PdO NP [38]. Reprinted with permissions from [32, 33, 36–38, 40]

Except for the SnO_2/Zn_2SnO_4 system, all nanoparticles have been deposited with a Haberland-type gas aggregation cluster source, which is described in more detail in the chapter "Memristive Switching: From Individual Nanoparticles Towards Complex Nanoparticle Networks" and allows for precise tailoring of alloy composition during deposition. In Fig. 8 a selection of gas sensors is depicted, with SEM micrographs showing the morphology and nanoparticle decoration, as well as characteristic gas sensor measurements.

The decoration with nanoparticles has shown to enhance the performance of MOS-based sensor devices. A thorough comparison of recent works can be found in [34]. A

deeper understanding of the participating interactions and mechanisms will allow for a tailored design of specialized or optimized material systems for sensor applications. As an example, the concept of the "electronic nose" can be realized by an array of highly selective and stable gas sensors, which is discussed as a valuable tool for the food industry or environmental applications [41, 42].

4 Triggered Assembly

The growing demand for computational power, arising from the development towards AI and the "Internet of Things" [2–4], as well as the resulting energy consumption will require highly efficient computer systems, with one of the main drawbacks of today's conventional computers being the losses of the von-Neumann architecture. A bio-inspired approach for a computing system based on the mammalian brain uses a low frequency but in a highly parallelized architecture in which memory, computation logic, energy source and cooling are decentralized. One challenge of such a complex system is the communication and thus the interconnections between the parallel components analogous to the connections between cortical regions of the brain [5]. In a brain interconnections are formed by closely timed spiking of neurons, called spike timing-dependent plasticity (STDP), which is, as a Hebbian learning rule, commonly summarized as "what fires together wires together". Neurons that spike in a window of a few milliseconds before another neuron nearby, potentiate the connection between these improving the efficiency of signal transmission [43]. On a technological level this concept can be transferred to a circuit of initially unconnected electronic components. Conductive interconnections between two nearby terminals are formed, if both are "active" during a narrow timeframe (but not simultaneously). This activity driven formation of conductive interconnections can be established by utilizing electrochemical metallization (ECM), where "activity" in this context is used to describe the potential of a terminal relative to a reference. The working principle of ECM cells is based on applying a voltage to electrodes where at least one of them consists of an electrochemically active material (e.g. Cu or Ag), which leads to a dissolution of metal ions into an electrolyte between the electrodes. The ions drift in the electrical field towards the cathode, where they are reduced and crystallize on the surface:

$$\begin{gathered} Anode : M \rightarrow M^{n+} + ne^{-} \\ \downarrow \quad Drift \quad \downarrow \\ Cathode : M^{n+} + ne^{-} \rightarrow M \end{gathered}$$

The crystallized metal forms a filament bridging the electrolyte thus reducing the resistance between the electrodes as long as the filaments holds. ECM is commonly used on the nanoscale as a memristive switching mechanism with an inert counter electrode and a solid electrolyte (e.g. SiO_2) [44, 45]. However, it is also possible to transfer this process to a larger length scale up to a range of several hundreds of

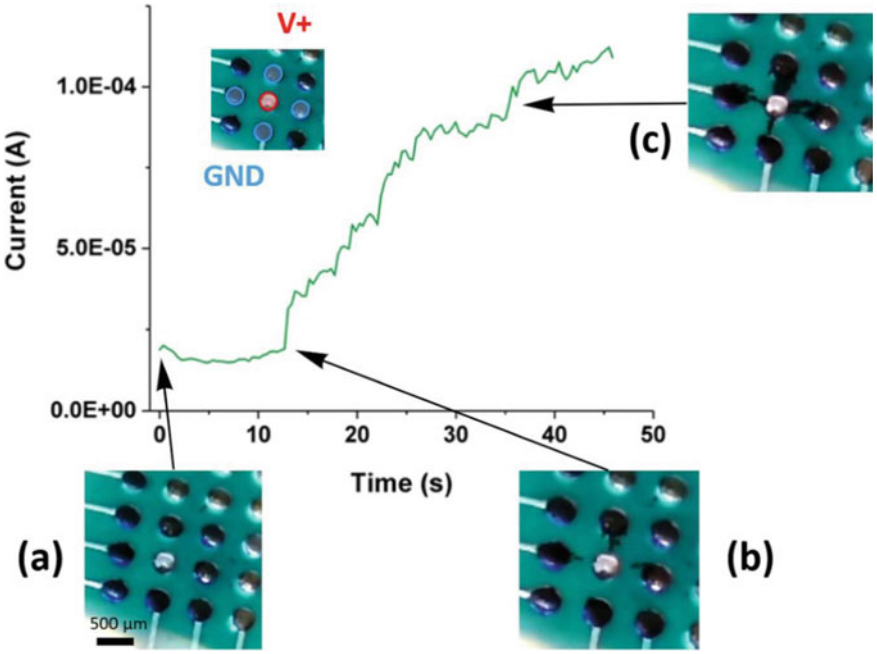

Fig. 9 Photographs and current measurement of an electrochemical metallization process over a dis-tance of 300 µm in an electrolyte of DMSO and MB with copper electrodes under an applied voltage of 15 V. The voltage has been applied to the center electrode. The perpendicular adja-cent electrodes have been connected to ground. All remaining ones were left floating. **a** In the beginning the current is determined by the conductivity of the electrolyte. **b** Filaments grow by metallization from cathode towards anode. The first filament establishing contact increases the conductance significantly. **c** Further growth leads to thicker filaments, gradually increas-ing the current

micrometers. Thus, filament growth by electrochemical metallization occurs as well for Cu electrodes with a spacing of 300 µm, when submerged in a liquid electrolyte of dimethyl sulfoxide (DMSO) and methylene blue (MB), which is shown in Fig. 9. By applying a voltage of 15 V to the central electrode and connecting ground to the adjacent ones, a metal filament has formed from cathode to anode directed by the electrical field, significantly increasing the conductance between them. EDX measurements revealed, that the filament formed consists of the electrode material, as seen in Fig. 10a+b. The liquid state facilitates ion mobility and allows for adjustment of electrolyte concentration, which can be used as parameter for the time constants of filament growth (see Fig. 10c).

If a periodic voltage signal is considered for a number of terminals oscillating around a resting potential, filament growth acts as positive feedback for closely but not exactly synchronized oscillators, since a large voltage drop will occur, where repeatedly one terminal is at its maximum while a nearby one is at its minimum. Thus, if the voltage magnitudes are properly set and two nearby terminals spike with similar (but not equal) frequencies over a sufficient period of time, they are

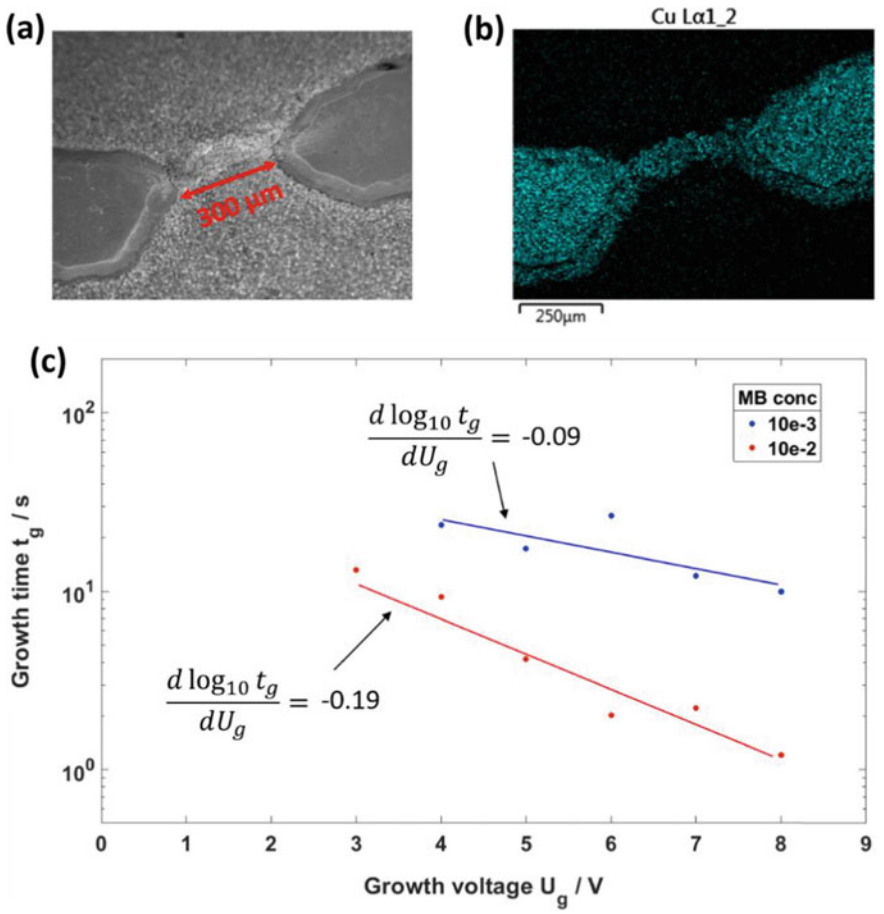

Fig. 10 **a+b** SEM micrograph and respective EDX map (Cu Lα1 signal) of two copper electrodes with grown filament. **c** Semi-logarithmic plot of time of filament growth over applied voltage for two electrolyte concentrations. The slope has been calculated by linear regression

interconnected by a metal filament drastically increasing the conductance between them. The growth time being in the second- to minute-scale acts as a low-pass filter, so that only those terminals are interconnected, that show a suitable potential drop consistently over a sufficient number of spikes. The larger length scale makes this approach a suitable base for integration into small-world setups and furthermore a combination with sensor devices allows the terminal activity to be driven by external stimuli.

5 Conclusion

The advance towards a data driven society with the "Smart City" and "Internet of Things" paradigms requires an ever growing demand of monitoring and sensing devices as well as imposing new challenges with respect to performance, energy efficiency and data processing but also design, scalability and fabrication of sensor devices. In this chapter various concepts have been discussed, tackling these challenges. A general model for a memsensor, whose equivalent circuit model consists of a stimulus dependent resistor (i.e. sensor) and two memristive components, has shown unique features like adaptation to a permanent background stimulus. It serves as a foundation for the interpretation of experimental findings and prediction of the behaviour of memsensitive devices, facilitating the development of smart, decentralized sensor systems. The unique features of memsensitive devices can be applied e.g. for monitoring the concentration of hazardous gases in a storage cabin. The sensor should not react to the slowly changing permanent background which is based on the number and kind of chemicals in the cabin, but only to quick changes such as when a container is damaged. Furthermore, it has been pointed out that additive manufacturing is a perfect candidate for the inexpensive, scalable fabrication of sensor devices with great design freedom in terms of geometry and material space as well as rapid iteration cycles. Microparticle based MOS-sensors have been shown as examples for sensor devices fabricated by DIW. An overview over various material system has been given, showcasing the enhancement of the performance, selectivity or stability of MOS-sensors by doping and decoration with nanoparticles, which allows for tailoring or designing sensor materials for specific applications. Finally, an approach is introduced for dynamically establishing conductive interconnections between metal electrodes in a liquid matrix. The concept is based on electrochemical metallization stimulated by voltage pulses. It acts as a self-organization mechanism to increase the conductance between active parts of a circuit resembling STDP. Using sensor devices, the "activity" can be driven by external stimuli, which offers a new way of introducing neuromorphic plasticity into sensor circuits.

References

1. Webster, M.A.: Evolving concepts of sensory adaptation. F1000 Biol. Rep. **4**, 21 (2012). https://doi.org/10.3410/B4-21
2. Zanella, A., et al.: Internet of things for smart cities. IEEE Internet Things J. **1**(1), 22–32 (2014). ISSN: 2327-4662. https://doi.org/10.1109/JIOT.2014.2306328
3. Bellavista, P., et al.: Convergence of MANET and WSN in IoT urban scenarios. IEEE Sens. J. **13**(10), 3558–3567 (2013). https://doi.org/10.1109/JSEN.2013.2272099
4. Atzori, L., Iera, A., Morabito, G.: The internet of things: a survey. Comput. Netw. **54**(15), 2787–2805 (2010). ISSN: 13891286. https://doi.org/10.1016/j.comnet.2010.05.010
5. Merolla, P.A., et al.: Artificial brains. A million spiking-neuron integrated circuit with a scalable communication network and interface. Science (New York, N.Y.) **345**(6197), 668–673 (2014). https://doi.org/10.1126/science.1254642

6. Khan, W.Z., et al.: Edge computing: a survey. Future Gener. Comput. Syst. **97**(99), 219–235 (2019). https://doi.org/10.1016/j.future.2019.02.050
7. Shaafiee, M., Logeswaran, R., Seddon, A.: Over-coming the limitations of von Neumann architecture in big data systems. In: Bansal, A., Singhal, A., (eds.), Proceedings of the 7th International Conference Confluence 2017 on Cloud Computing, Data Science and Engineering, pp. 199–203. IEEE, Piscataway (2017). isbn: 978-1-5090-3519-9. https://doi.org/10.1109/CONFLUENCE.2017.7943149
8. Kendall, J.D., Kumar, S.: The building blocks of a brain-inspired computer. Appl. Phys. Rev. **7**(1), 011305 (2020). ISSN: 1931–9401. https://doi.org/10.1063/1.5129306
9. Zou, L., et al.: Novel tactile sensor technology and smart tactile sensing systems: a review. Sensors (Basel, Switzerland) **17**(11) (2017). https://doi.org/10.3390/s17112653
10. Nazemi, H., et al.: Advanced micro- and nano-gas sensor technology: a review. Sensors (Basel, Switzerland) **19**(6) (2019). https://doi.org/10.3390/s19061285
11. Vahl, A., et al.: Concept and modelling of memsensors as two ter-minal devices with enhanced capabilities in neuromorphic engineering. Sci. Rep. **9**(1), 4361 (2019). https://doi.org/10.1038/s41598-019-39008-5
12. Chiolerio, A., et al.: Ultraviolet mem-sensors: Flexible anisotropic composites featuring giant photocurrent enhancement. In: Nano Res. **8**(6), 1956–1963 (2015). ISSN: 1998-0124. https://doi.org/10.1007/s12274-014-0705-2
13. Wang, X., et al.: Spintronic memristor temperature sensor. IEEE Electron Device Lett. **31**(1), 20–22 (2010). ISSN: 0741-3106. https://doi.org/10.1109/LED.2009.2035643
14. Li, H., et al.: Light and magnetic field double modulation on the resistive switching behavior in $BaTiO_3$ /FeMn/$BaTiO_3$ trilayer films. Phys. Lett. A **381**(25–26), 2127–2130 (2017). ISSN: 03759601. https://doi.org/10.1016/j.physleta.2017.04.039
15. Ngo, T.D., et al.: Additive manufacturing (3D printing): a review of ma-terials, methods, applications and challenges. Compos. Part B: Eng. **143**(2), 172–196 (2018). ISSN: 13598368. https://doi.org/10.1016/j.compositesb.2018.02.012
16. Kaufui V. Wong and Aldo Hernandez. "A Review of Additive Manufacturing. In: ISRN Mechanical Engineering 2012.4 (2012), pp. 1–10. ISSN: 2090-5130. https://doi.org/10.5402/2012/208760
17. Lewis, J.A.: Direct ink writing of 3D functional materials. Adv. Funct. Mater. **16**(17), 2193–2204 (2006). https://doi.org/10.1002/adfm.200600434
18. Lewis, J.A.: Direct-write assembly of ceramics from colloidal inks. Current Opinion Solid State Mater. Sci. **6**(3), 245– 250 (2002). ISSN: 13590286. https://doi.org/10.1016/S1359-0286(02)00031-1
19. Rueschhoff, L., et al.: Additive manufacturing of dense ceramic parts via direct ink writing of aqueous alumina suspensions. Int. J. Appl. Ceram. Technol. **13**(5), 821–830 (2016). https://doi.org/10.1111/ijac.12557
20. Paulowicz, I., et al.: Zinc oxide nanotetrapods with four different arm mor-phologies for versatile nanosensors. Sens. Actuat. B: Chem. **262**, 425–435 (2018). ISSN: 09254005. https://doi.org/10.1016/j.snb.2018.01.206
21. Wagner, S., et al.: Electronic skin: architecture and components. Phys. E: Low-dimensional Syst. Nanostruct. **25**(2–3), 326–334 (2004). ISSN: 13869477. https://doi.org/10.1016/j.physe.2004.06.032
22. Wang, X., et al.: Recent progress in electronic skin. Adv. Sci. (Weinheim, Baden-Wurttemberg, Germany) **2**(10), 1500169 (2015). ISSN: 2198-3844. https://doi.org/10.1002/advs.201500169
23. Ji, H., Zeng, W., Li, Y.: Gas sensing mechanisms of metal oxide semiconductors: a focus review. Nanoscale **11**(47), 22664–22684 (2019). https://doi.org/10.1039/c9nr07699a
24. Anderson, J.C.: Measuring breath acetone for monitoring fat loss: review. Obesity (Silver Spring, Md.) **23**(12), 2327–2334 (2015). https://doi.org/10.1002/oby.21242
25. Saasa, V., et al.: Sensing technologies for detection of acetone in human breath for diabetes diagnosis and monitoring. Diagnostics (Basel, Switzerland) **8**(1) (2018). ISSN: 2075-4418. https://doi.org/10.3390/diagnostics8010012

26. Lupan, O., Siebert, L.: 3D-printed chemiresistive sensor array on nanowire CuO/Cu_2O/Cu heterojunction nets. ACS Appl. Mater. Interfaces (2019)
27. Siebert, L., et al.: Facile fabrication of semiconducting oxide nanostruc-tures by direct ink writing of readily available metal microparticles and their application as low power acetone gas sensors. Nano Energy **70**(2), 104420 (2020). ISSN: 22112855. https://doi.org/10.1016/j.nanoen.2019.104420
28. Lupan, O., et al.: Selective hydrogen gas nanosensor using individual ZnO nanowire with fast response at room temperature. In: Sens. Actuat. B: Chem. **144**(1), 56–66 (2010). ISSN: 09254005. https://doi.org/10.1016/j.snb.2009.10.038
29. Lupan, O. et al.: Highly sensitive and selective hydrogen single-nanowire nanosensor. Sens. Actuat. B: Chem. **173**(3) 772–780 (2012). ISSN: 09254005. https://doi.org/10.1016/j.snb.2012.07.111
30. Lupan, O. et al.: Room temperature gas nanosensors based on individual and multiple networked Au-modified ZnO nanowires. In: Sens. Actuat. B: Chem. **299**, 126977 (2019). ISSN: 09254005. https://doi.org/10.1016/j.snb.2019.126977
31. Lupan, O. et al.: Low-temperature solution synthesis of Au-modified ZnO nanowires for highly efficient hydrogen nanosensors. In: ACS Applied Materials and Interfaces (2019). https://doi.org/10.1021/acsami.9b08598
32. Postica, V., et al.: Tuning doping and surface functionalization of columnar oxide films for volatile organic compound sensing: experiments and theory. J. Mater. Chem. A **6**(46) 23669–23682 (2018). ISSN: 2050-7488. https://doi.org/10.1039/c8ta08985j
33. Postica, V., et al.: Tuning ZnO sensors reactivity toward volatile organic compounds via Ag doping and nanoparticle functionalization. ACS Appl. Mater. Interfaces **11**(34), 31452–31466 (2019)
34. Vahl, A., et al.: Surface functionalization of ZnO: Ag columnar thin films with AgAu and AgPt bimetallic alloy nanoparticles as an efficient path-way for highly sensitive gas discrimination and early hazard detection in batteries. J. Mater. Chem. A **8**(32), 16246– 16264 (2020). ISSN: 2050-7488. https://doi.org/10.1039/d0ta03224g
35. Lupan, O., et al.: Ultra-thin TiO 2 films by atomic layer deposition and surface functionalization with Au nanodots for sensing applications. Mater. Sci. Semiconduct. Process. **87**, 44–53 (2018). ISSN: 13698001. https://doi.org/10.1016/j.mssp.2018.06.031
36. Ababii, N., et al.: Effect of noble metal functionalization and film thickness on sensing properties of sprayed TiO2 ultra-thin films. Sens. Actuat. A: Phys. **293**, 242–258 (2019). ISSN: 09244247. https://doi.org/10.1016/j.sna.2019.04.017
37. Lupan, C., et al.: Pd-functionalized ZnO: Eu columnar films for room-temperature hydrogen gas sensing: a combined experimental and com-putational approach. ACS Appl. Mater. Interfaces **12**(22), 24951–24964 (2020). https://doi.org/10.1021/acsami.0c02103
38. Lupan, O., et al.: PdO/PdO2 functionalized ZnO: Pd films for lower operating temperature H2 gas sensing. Nanoscale **10**(29), 14107–14127 (2018). https://doi.org/10.1039/c8nr03260b
39. Lupan, O. et al.: Functionalized Pd/ZnO nanowires for nanosensors. Physica Status solidi (RRL) - Rapid Res. Lett. **12**(1), 1700321 (2018). ISSN: 18626254. https://doi.org/10.1002/pssr.201700321
40. Lupan, O. et al.: Properties of a single SnO2: Zn2SnO4 – functional-ized nanowire based nanosensor. Ceram. Int. **44**(5), 4859–4867 (2018). ISSN: 02728842. https://doi.org/10.1016/j.ceramint.2017.12.075
41. Wilson, A., Baietto, M.: Applications and advances in electronic-nose technologies. Sensors **9**(7), 5099–5148 (2009). ISSN: 1424-8220. https://doi.org/10.3390/s90705099
42. Boeker, P.: On 'Electronic Nose' methodology. Sens. Actuat. B: Chem. **204**, 2–17 (2014). ISSN: 09254005. https://doi.org/10.1016/j.snb.2014.07.087
43. Caporale, N., Dan, Y.: Spike timing-dependent plasticity: a Heb-bian learning rule. In: Annual Review of Neuroscience, vol. 31, pp. 25–46 (2008). ISSN: 0147-006X

44. Valov, I., et al.: Electrochemical metallization memories—fundamentals, applications, prospects. Nanotechnology **22**(28), 289502 (2011). ISSN: 0957-4484. https://doi.org/10.1088/0957-4484/22/28/289502
45. Peng, S., et al.: Mechanism for resistive switching in an oxide-based electrochemical metallization memory. Appl. Phys. Lett. **100**(7), 072101 (2012). ISSN: 0003-6951. https://doi.org/10.1063/1.3683523